Chapter 3

Testing the nature of the ULX source in Holmberg II with *AstroSat*

3.1 Introduction

In the preceding chapter, we discussed how the remarkable enhancement in the resolution of the *AstroSat*/UVIT instrument has facilitated the identification of distinct point sources. This improvement, notably highlighted the detectability of the ULX source Ho II X-1, a significant advancement over its predecessor, *GALEX*. Consequently, in this chapter, our focus shifts towards comprehending the nature of emissions emanating from the ULX. ULX sources, by definition, are extragalactic point-like sources with non-nuclear origin, showcasing apparent luminosities surpassing the Eddington limit characteristic of typical black holes within our galaxy. Notably, these sources show considerable variability both in the X-ray spectrum and the UV/optical wavelengths. Herein, we present the X-ray observations of Ho II, conducted simultaneously with the UV observations discussed in the previous chapter. Our objective was to identify the flux variability exhibited by the object across both UV and X-ray spectrums, aiming to discover any correlation between them. Additionally, we discussed several plausible models capable of generating such a correlation.

3.2 Ultra luminous X-ray sources (ULX)

As previously mentioned, ULXs are distinct non-nuclear, point-like sources found beyond our galaxy, displaying luminosities that surpass the Eddington limit typical for black holes within our own Milky Way. According to contemporary understanding, most of these sources are believed to be binary systems, housing either stellar-mass black holes or neutron stars

that accrete material at rates exceeding the Eddington limit [123, 124]. The identification of neutron stars within ULXs became apparent following the discovery of coherent pulsations within the X-ray emissions of the renowned ULX source M82 X-2 [125]. Subsequently, the recognition of approximately a dozen ultraluminous pulsars (ULXPs) has solidified this understanding.

Supercritical accretion, a hallmark of super-Eddington accretion, prominently features strong outflows stemming from the innermost regions of the accretion disk [126]. These outflows have been spectroscopically observed across both X-ray and optical spectra, revealing intriguing distinctions in their properties between the two ranges. In the X-ray spectrum, the spectral lines originating from the outflowing matter exhibit pronounced blueshifts, indicative of gas velocities reaching approximately $0.1c$, denoting ultra-fast outflows [127]. Conversely, within the optical range, the outflow resembles stellar winds, exhibiting velocities spanning $500 - 1500$ km/s [128]. This optical wind is believed to be optically thick, potentially forming an extensive photosphere enveloping the supercritical accretion disk. Employing modeling techniques similar to those used for analyzing the optical spectra of Wolf-Rayet and LBV stars, investigations have estimated the mass loss rate within the ULX wind to range between $10^{-6} - 10^{-5.5}$ $M_{\odot}$/yr [129].

To ascertain the required accretion rates, it's crucial that the donor star resides within a close orbit, likely filling its Roche lobe — a characteristic noted in the initial discovery of the donor star in M101 ULX-1, a Wolf-Rayet star [130]. While donor stars have been identified in only a few ULXs, they are predominantly observed as blue or red supergiants [131–135]. However, despite this, a substantial portion of the optical emission is believed to originate not from the donor stars themselves but rather from the wind photosphere surrounding the supercritical disk ([124], and references therein). Studies have revealed intriguing spectral energy distributions (SEDs) within ULXs. The brightest sources in the optical range exhibit blue, power-law SEDs, peaking in the FUV band beyond the observable wavelength range [136–138]. Conversely, less luminous ULXs display SEDs consistent with the spectra of A-G class stars [139, 140]. This observation implies that while the brightest ULX counterparts are largely dominated by optical emissions from the hot supercritical accretion disk, the prominence of donor star emission becomes more apparent as the contribution from the disk decreases [141].

It is assumed that the optical radiation emitted by the supercritical disk originates from the reprocessing of X-ray quanta in the outer regions of the accretion disk or within the wind

[128, 142]. This optical emission's intensity ratio, relative to X-ray emissions, can significantly vary depending on the specific characteristics of the region where the hard quanta are re-emitted and the inclination angle of the accretion disk with respect to the observer's line of sight. Consequently, a collective analysis of both optical and X-ray emissions from ULXs becomes crucial. Such investigations hold the potential to uncover details concerning wind formation and outflow geometry. Initial progress in this area has been made; for instance, [137] conducted simultaneous observations of NGC 5408 X-1 using the *Chandra X-ray Observatory* and the *HST*, constructing the source's SED spanning wavelengths from X-rays to NIR. However, limited variability observed during these observations hindered the authors' ability to test for potential correlations between emissions across these bands.

For few transient ULX sources, reliable correlations between UV-optical and X-ray fluxes have been reported. For instance, in case of UGC 6456 ULX, a positive correlation was seen not only between X-rays and broadband optical emissions but also indirectly extended to the flux observed within the HeII λ4686 emission line [143]. Nevertheless, due to the limited number of observations available, the underlying physical mechanisms responsible for the observed variability across diverse wavelengths was not extensively considered. Hence, in this work, we aim to address this gap by utilizing multiple simultaneous X-ray and UV observations of the ULX source Ho II X-1. Our objective is to detect any potential correlation between these emissions and understand the physical mechanisms that might be responsible for this correlation.

3.3 X-ray observations

AstroSat is equipped with three instruments for X-ray observations across different energy ranges. The Soft X-ray Telescope (SXT) operates within the energy span of $0.3 - 8$ keV, providing X-ray images and spectra. Utilizing focusing optics of the Wolter-I type and a CCD camera similar to those found in the XMM and *Swift* missions, the SXT provides an effective area of 200 cm^2 at 1.5 keV and functions with a 2-meter focal length. It offers a point spread function (PSF) ranging between $3'$–$4'$, a half-power diameter (HPD) of $10'$, and a telescope field of view of $\approx 40'$. In scenarios involving observations of faint sources, the detector operates in photon counting mode, delivering a time resolution of 2.4 seconds. The other two detectors, the Large Area X-ray Proportional Counter (LAXPC) utilizing xenon-filled proportional counters, and the Cadmium Zinc Telluride Imager (CZTI) employing a pixellated cadmium-zinc-telluride array with a coded aperture mask, cover energies within the 10 to 150 keV range. Despite the LAXPC's significant effective area (approximately

Table 3.1 Observation dates, exposures and measured source fluxes. The X-ray fluxes (0.7-7.0 keV) are in units of 10^{-12} erg s^{-1} cm^{-2}. The UV flux densities (background subtracted) are in units of 10^{-16} erg s^{-1} cm^{-2} Å^{-1}

Obs No.	ObsID	Start time Stop time	Channel (filter)	Flux	$T_{\rm exp}$, ks
1	G05_204T01_9000000688	2016-09-29 11:05:10 2016-09-30 18:00:59	SXT F148W N279N	5.6 ± 0.4 2.03 ± 0.23 0.85 ± 0.07	32.8 11.2 10.6
2	A02_046T01_9000000814	2016-11-21 10:05:38 2016-11-21 19:02:48	SXT F154W N245M	6.2 ± 0.6 2.30 ± 0.28 1.20 ± 0.03	11.8 9.0 8.2
3	A02_046T01_9000000864	2016-12-08 16:09:32 2016-12-09 09:25:44	SXT F154W N245M	6.3 ± 0.7 1.91 ± 0.27 1.11 ± 0.04	13.0 9.1 8.7
4	A07_054T01_9000003286	2019-11-06 13:40:15 2019-11-07 16:08:24	SXT	7.0 ± 0.6	18.6
5	A07_054T01_9000003348	2019-11-30 20:04:51 2019-12-01 18:19:17	SXT	6.4 ± 0.5	22.8
6	A07_054T01_9000003370	2019-12-16 12:10:41 2019-12-17 13:01:34	SXT F148W	7.7 ± 0.5 2.27 ± 0.23	24.0 17.4
7	A07_054T01_9000003378	2019-12-19 23:11:21 2019-12-21 07:44:29	SXT F148W	6.9 ± 0.5 2.39 ± 0.23	26.8 17.2
8	A07_054T01_9000003406	2020-01-02 00:36:10 2020-01-02 22:55:01	SXT F148W	6.9 ± 0.5 2.12 ± 0.20	23.0 16.8
9	A07_054T01_9000003486	2020-02-07 17:18:19 2020-02-08 18:48:29	SXT F148W	7.0 ± 0.5 2.11 ± 0.24	23.1 16.6
10	A07_054T01_9000003504	2020-02-15 08:58:50 2020-02-16 08:34:22	SXT F148W	6.5 ± 0.5 2.04 ± 0.23	23.2 17.1

6000 cm^2), its spatial resolution is poor, leading to high background levels. Consequently, these detectors prove inefficient for observing extragalactic sources like ULXs. Moreover, observations conducted with *NuStar* have revealed a sharp decline in the X-ray flux of ULXs beyond 15–20 keV. After assessing the LAXPC data, it was evident that the signal remaining post-background subtraction held minimal statistical significance across all Ho II X-1 observations. Consequently, we opt not to include the LAXPC and CZTI data within our analysis. The details of the *AstroSat* X-ray observations with SXT, along with the source fluxes of Ho II X-1 in both X-ray and UV (for UV observation, see 2.2.2 in Chapter 2) is provided in Table 3.1. For the reduction of X-ray data, please consult [114], as this aspect was undertaken by my collaborators in the paper and not by myself.

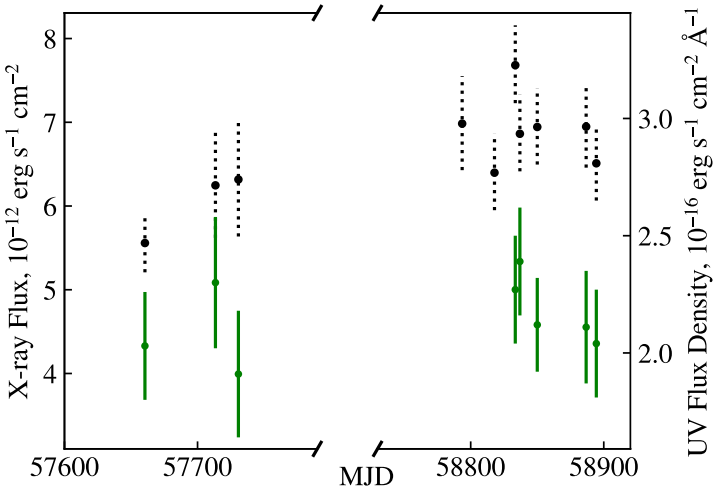

Fig. 3.1 Light curve of synchronous X-ray–UV observations of Ho II X-1. The X-ray fluxes (0.7–7 keV) are marked by black points with dashed bars; the UV flux densities at 148.1 nm (F148W filter), are shown in green

3.4 Results and Discussions

In X-ray, *AstroSat* observed Ho II X-1 10 times from September 2016 to February 2020, whereas in X-ray and UV simultaneously, it was observed 8 times. Over all these observations, the object have demonstrated a rather weak variability in both the X-ray and UV ranges. The maximum scatter in X-rays is about 1.5 times (between Obs 1 and 6). [144] noted that fast variations of the X-ray flux do not lead to spectral changes. It has been proposed that apparent flux variations may be produced by relatively cold gas clouds which diminish the X-ray radiation for the observer intersecting line of sight [145, 146].

The averaged over all the observations source luminosity is $L_{0.7-7\,\mathrm{keV}} \approx 8 \times 10^{39}$ erg s^{-1} (assuming isotropic emission and distance of 3.39 Mpc). In the UV range, the mean flux density in the F148W filter ($\approx$ 1500 Å) is $F_{\mathrm{F148W}} = 2.15 \times 10^{-16}$ erg s^{-1} cm^{-2} Å^{-1}, that correspond to luminosity of $L_{\mathrm{F148W}} = 1.30 \times 10^{38}$ erg s^{-1} calculated using effective bandwidth of F148W filter. The variability amplitude is about 25% of the minimum value which only slightly exceeds the 2-σ errors of the individual measurements. The χ^2 test against the null-hypothesis of constant flux yields a p-value of ≈ 0.89, it means that the detected variability is not significant, and we can only speak about its upper limit.

In Fig. 3.2 we plot the X-ray fluxes against the UV flux densities at $\approx$ 1500Å. Due to high uncertainties in both the X-ray and UV bands, the relationship between the data points is not visible, nevertheless, the correlation between these two bands caused by heating of

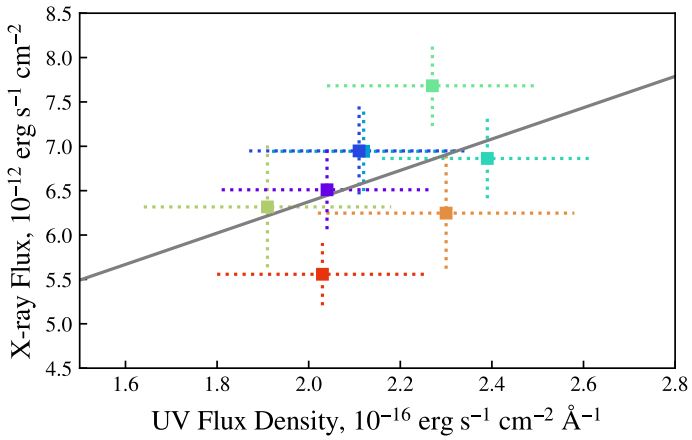

Fig. 3.2 X-ray fluxes against UV flux densities at 148.1 nm (F148W filter). Colors are in the rainbow order from red (observation #1) to violet (#10). Formal Pearson correlation coefficient is $R = 0.45$

different gas structures by X-ray quanta is predicted by many ULX models. The X-ray radiation has to come from areas in close vicinity to the accretor. It may be inner parts of the supercritical accretion disk or/and a hot optically thick gas envelope if the accretor is a highly magnetized neutron star [147]. The heating may affect an optically thick wind coming from the supercritical disk [126], distant parts from the disk itself or the donor star. The presence of the wind emitting in the UV/optical range is proven by both the 2D MHD simulations [148] and the observed optical spectra of ULXs [128] which require the wind in order to describe a plenty of emission lines typical for them [129, 149]. Below all three options will be considered.

Even if the initial accretion rate in a disk is $\dot{M}_0 \gg \dot{M}_{\rm Edd}$, its far regions that emit in the UV/optical band still release not much energy and, therefore, are supposed to be very similar to those of the standard, subcritical ones [126]. It has been shown that for the subcritical geometrically thin disks around low-mass X-ray binaries, the UV-optical variability induced by heating should be $F_{\rm UV} \propto L_{\rm X}^{\alpha}$ with $\alpha \sim 0.5$ [142, 150]. According to this, the X-ray flux changes by 1.5 times found by *AstroSat* should correspond to the UV variability of 20–30%. This is close to that we have observed.

The optical and IR emission of the supercritical disk wind should have a steeper dependence on the X-ray luminosity [128]. It is due to luminosity in these ranges, being related to the Rayleigh-Jeans regions of the wind spectra, is determined mainly by the size of the emitting structure which is not constant as in the case of the standard disk but depends roughly linearly on the initial accretion rate $\dot{M}_0$. The higher the accretion rate, the wind stronger

and its photosphere larger and colder; the maximum of the emitted spectrum is then shifted towards longer wavelengths [124]. The X-ray luminosity, in turn, depends logarithmically on $\dot{M}_0$ [151, 126]. Nevertheless, the size of the wind region that emits in the UV range remains almost unchanged because the increase of $\dot{M}_0$ just creates new colder wind parts beyond this region. Thus we can conclude that the supercritical disk wind should demonstrate the similar dependence $F_{\rm UV} \propto L_{\rm X}^{0.5}$.

To assess UV flux variations due to heating of the donor, we carried out a modeling with following assumptions. Since the result have to strongly depend on the initial temperature T_0 of the star surface, we have considered two stars: B2 Ib and O8 Ib, that were proposed by [136] as possible donors of Ho II X-1. In this study, the authors analyzed the UV and X-ray spectroscopic data of the ULX source using data from *HST* and *X-ray Multi-Mirror Mission (XMM)*, respectively. They fitted the data with various stellar models and suggested that the UV/optical emission from Ho II X-1 might primarily result from an X-ray irradiated disk. The accretor was either a black hole (BH) of 10 $M_\odot$ or a neutron star (NS) of 1.5 $M_\odot$. The source of X-ray quanta was assumed to be point-like, the donor fills its Roche lobe, the size of which was computed via the relations by [152]. The masses, effective temperatures and radii (20.0 $M_\odot$, 20.3 kK, 23.2 $R_\odot$ and 52.5 $M_\odot$, 34.3 kK, 20.4 $R_\odot$ for the B2 Ib and O8 Ib star, respectively) were taken from [153]. The orbit of the system was assumed to be circular with a separation determined from the condition of Roche lobe filling. The observed flux density from i-th element of the star surface was computed using the Planck function with a temperature found from equation:

$$\sigma T_{{\rm new},i}^4 = \sigma T_0^4 + (1-\varepsilon)\cos\beta_i F_i \tag{3.1}$$

where F_i — irradiating flux, β_i — the angle between the directions to the X-ray source and the surface element normal, the albedo ε was assumed to be 0.5 [154]. In Fig. 3.3 we show the new temperatures averaged over the visible disk of the star and the total flux densities at 1500 Å (very close to λ_c of the F148W filter) normalized to the values not modified by heating as functions of the X-ray luminosity. Besides two types of the donor and two types of the accretor we also considered two orientations: with the orbit inclination $i = 0$ and $i = i_{\max}$ that was calculated individually for each case (for a particular star size and binary separation, see the figure legend) to satisfy the condition of the system being non-eclipsing in X-rays. In the later case the donor was behind the X-ray source to make the observed effect as large as possible; the option $i = 0$ was considered because majority of ULX models predicts that such systems must be viewed nearly along its axis to prevent covering of inner parts of the

accretion disk by gas flows.

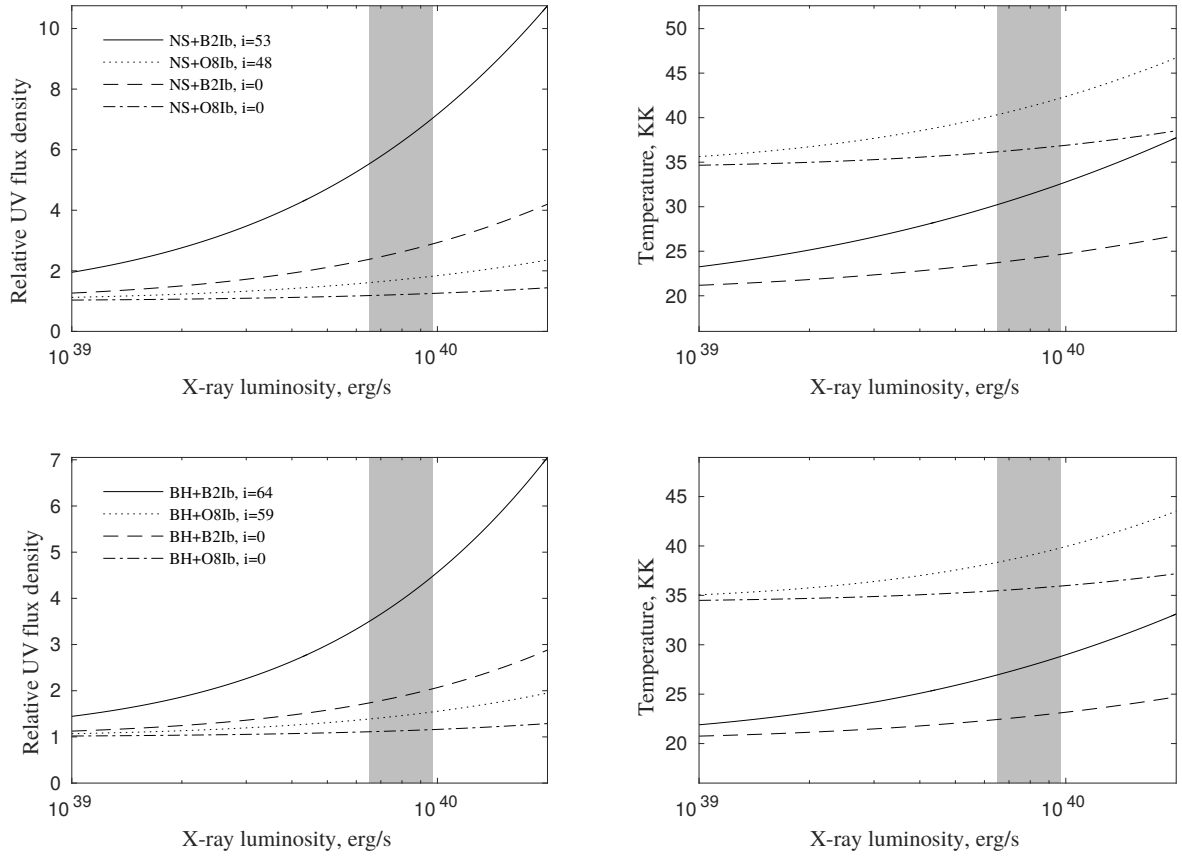

Fig. 3.3 The ratio of the flux densities at 1500 Å from the heated and not heated donors (*left panels*), and the temperatures averaged over the visible star disk (*right panels*) as functions of the X-ray luminosity of the accretor. Two type of the accretors: a neutron star (*top*) and a black hole (*bottom*) are considered. The donor is either a O8 or B2 supergiant. The orbit inclination either $i = 0$ (view along the axis) or the maximum possible angle at which the particular system remains non-eclipsing in X-rays. Grey areas show the range of Ho II X-1 X-ray luminosities in the *AstroSat* observations

As it is seen from Fig. 3.3, the systems with a neutron star should yield more prominent increase of the UV flux due to their compactness. The maximal UV flux variations of $\approx$ 27–28% (for the X-ray luminosities from 6.5×10^{39} to 9.7×10^{39} erg s^{-1} found by *AstroSat*) occurs with the B2 Ib star regardless the accretor type. In the other cases, the variations is less, $\sim$ 20%, with a minimum $\approx$ 4% shown by the BH+O8 Ib system viewed from its pole. At the same time, the heated B2 Ib star gives correct temperatures (close to that approximated by [136] for Ho II X-1) only with a NS viewed at $i_{\max}$ (maximal heating). The

O8 Ib star, in contrast, gives the correct temperature in all the cases except 'NS with $i_{\max}$'. Thus, the observed SED temperature and low variability amplitude in the UV range make the hotter donor more preferable. Nevertheless, we should note that we did not consider the orbital variations in this modeling. This effects, however, can be important only for systems seen nearly along the orbital plane which is thought to be unlikely for ULXs. Also, the observed variations of the X-ray flux may be caused by effects of shielding of the X-ray source by cold opaque clouds/gas flows without changing the true luminosity and, hence, the irradiating flux as well. This effects should reduce the UV variability predicted by the models.

In light of the above, one can see that the UV variability amplitudes predicted by all three considered models do not contradict the observed value due to its large uncertainties. Therefore, we have estimated the minimal required variability level in both ranges that would allow to distinguish the models. We assumed that variability could by considered as significant when at least one of data points bounces 3σ up and one 3σ down from the averaged flux. Since the UVIT uncertainties is about 10%, the UV variability must be at least 60% to be considered as firmly detected. For the disk/wind heating models this correspond to the X-ray variations with a factor of $\gtrsim 2.5$. So, if one detects a variability of this level in X-rays but none in the UV band, it could be concluded the UV radiation is dominated by a heated O-type donor because this star have to provide the UV variability of $\lesssim 30\%$ regardless the accretor type and orbit inclination.

3.5 Conclusions

The Indian space satellite *AstroSat* observed Ho II X-1 in ten epochs, eight of them simultaneously in the X-ray and UV bands. The *AstroSat* payload is similar to that of *Swift* which also have an UV/optical telescope but the spatial resolution of the *AstroSat*/UVIT is twice better. This allows to study optical counterparts of the X-ray sources residing in crowded stellar fields.

Though Ho II X-1 is known as one of the most variable sources among the bonafide ULXs (with a factor up to 13 [144]), we were unlucky to catch it in a state of low variability. We found only 1.5 times in X-rays and about 25% (upper limit) in the UV band, which did not allow us to detect tight correlation between this bands predicted by different models. We have considered three models of heating: the heated thin disk, the wind or the O-B supergiant donor star, but cannot reject any of them with the observed variability level. To distinguish the models, we estimate the required X-ray variability as ~ 2.5 or higher. Our short glance on

recent *Swift* observations have shown that the object returned to the state of high variability since February 2021. This gives hope that further *AstroSat* observations will finally detect the correlation and will help to clarify the nature of the Ho II X-1 UV-optical emission.